



Contents lists available at *Avicenna Publishing Corporation (APC)*

Asian Journal of Green Chemistry

Journal homepage: www.ajgreenchem.com



Original Research Article

Silver functionalized on hydroxyapatite-core-shell magnetic γ - Fe_2O_3 : An environmentally and readily recyclable nanocatalyst for the one-pot synthesis of 14H-dibenzo[a,j]xanthenes derivatives

Zeinab Arzehgar^{a,*} , Abdelkarim Aydi^b , Mohammad Mirzaei Heydari^c

^a Department of Chemistry, Payame Noor University, PO BOX 19395-4697 Tehran, Iran

^b Department of Chemical and Materials Engineering, College of Engineering, National College of Chemical Industry, Nancy, Polytechnic Institute of Lorraine, France Frankfurt Am Main Area, Germany

^c School of Environment, Natural Resources & Geography, Bangor University, Bangor, Gwynedd, Wales, United Kingdom

ARTICLE INFORMATION

Received: 4 April 2018

Received in revised: 8 April 2018

Accepted: 8 April 2018

Available online: 13 May 2018

DOI: [10.22034/ajgc.2018.61867](https://doi.org/10.22034/ajgc.2018.61867)

KEYWORDS

γ - Fe_2O_3 @HAp-Ag

Lewis acidic catalyst

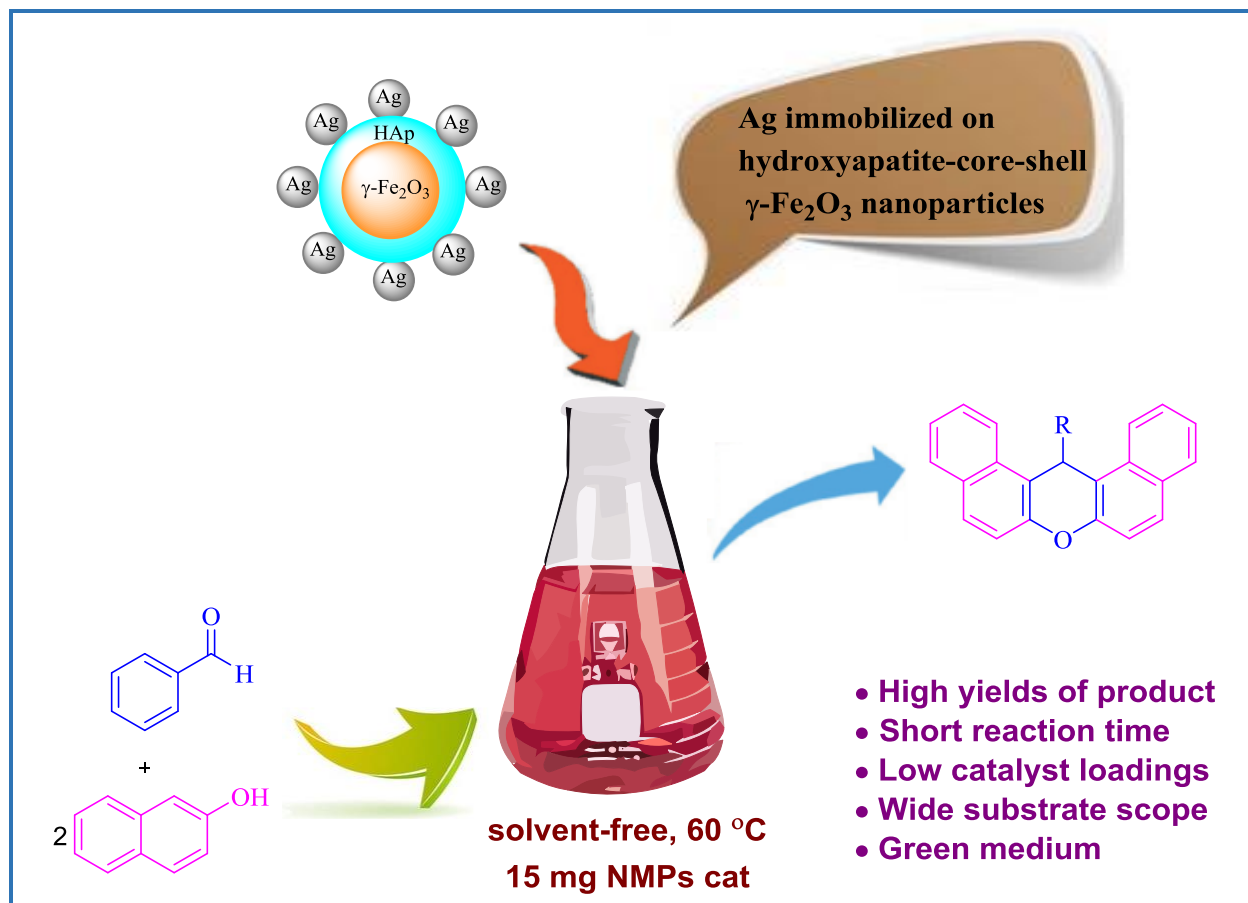
14-aryl-14Hdibenzo[a,j]xanthenes

Reusable of catalyst

ABSTRACT

An efficient and simple procedure for the preparation of silver functionalized on hydroxyapatite-core-shell magnetic γ - Fe_2O_3 nanoparticles (γ - Fe_2O_3 @HAp-Ag) as an environmentally efficient magnetically recoverable and reusable catalyst is described, and it is used for the one-pot synthesis of 14-aryl-14H-dibenzo[a,j]xanthenes *via* a cost-effective and atom-economical procedure from substituted benzaldehydes and β -naphthol under solvent-free conditions at 60 °C. The attractiveness of this protocol lies in its green approach in that the catalyst is easily recoverable using an external magnet, which makes the process economical.

Graphical Abstract



Introduction

Xanthenes and Benzoxanthenes are an important category of organic compounds which recently received much attention of organic and medical chemists due to of their wide range of therapeutic and biological properties such as antifungal [1], antibacterial [2] and anti inflammatory activities [3]. Furthermore, these compounds in laser technologies [4], fluorescent material of visualization of biomolecules [5] and have been widely used as dyes [6]. Many methods using the synthesis of xanthene and benzoxanthene have been reported in the literature, including cyclodehydration [7–10], cyclization of polycyclic aryl triflate esters [11], trapping of benzyne by phenols [12], Intermolecular phenyl carbonyl coupling reactions of benzaldehydes and acetophenones [13] and cyclocondensation between 2-hydroxy aromatic aldehydes and 2-tetralone [14]. The synthesis process of the xanthenes has been improved by condensing of aldehydes and 2-naphthol in the presence of an acid catalyst such as ZnO-NPs [15], selectfluor™ [16], sulfamic acid [17], Imidazol-1-yl-acetic acid [18], succinimide-*N*-sulfonic acid [19], montmorillonite K10 [20], sulfonic acid

functionalized imidazolium salts (SAFIS) [21], Ferric Hydrogensulfate [22], 2,6-Pyridinedicarboxylic acid [23], $\gamma\text{-Fe}_2\text{O}_3\text{@HAp-Fe}^{2+}$ [24] and silica-bonded imidazolium-sulfonic acid chloride (SBISAC) [25]. Furthermore, most of the reported methods for the synthesis of the title compounds are associated with one or more of the following drawbacks: low yields, long reaction times, the use of large amount of catalyst, and the use of expensive, non-available or toxic catalysts, tedious work-up procedure, performances under certain special conditions, and poor agreement with the green chemistry protocols.

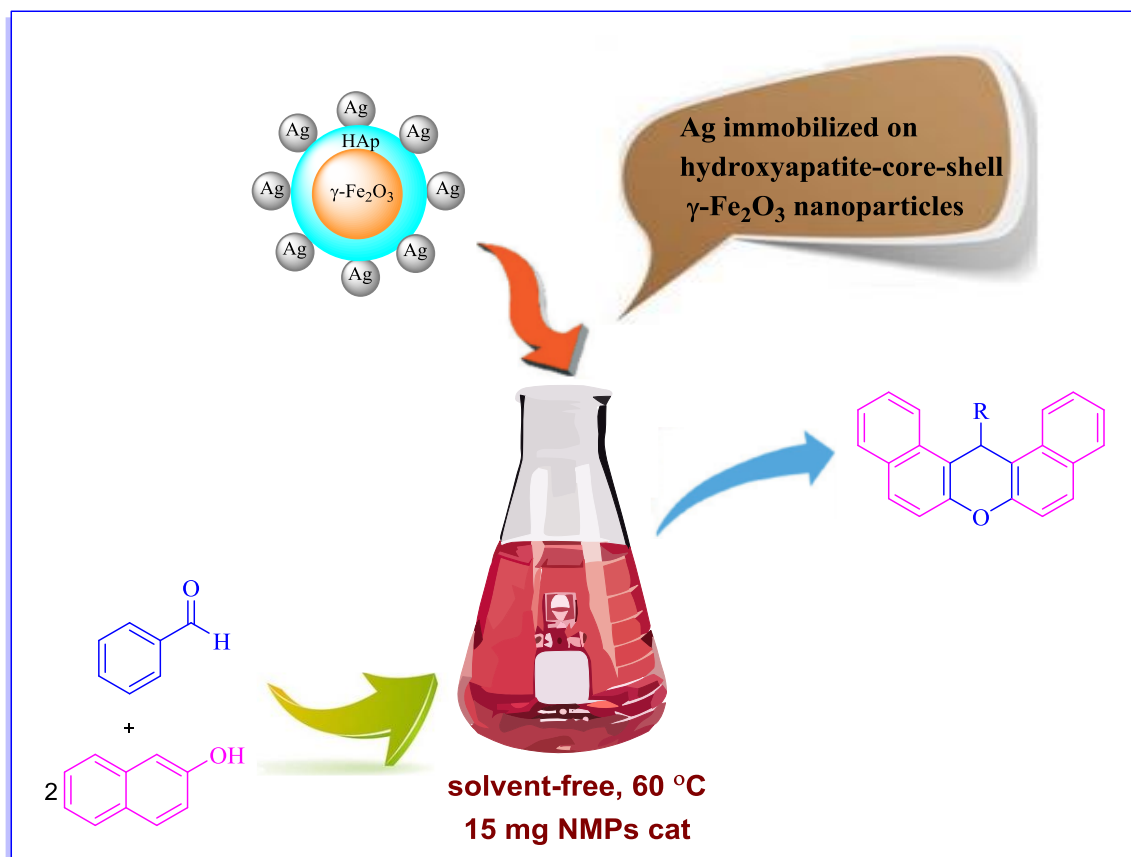
Fe^{2+} , Ni^{2+} , and Ag functionalized on hydroxyapatite-core-shell $\gamma\text{-Fe}_2\text{O}_3$ ($\gamma\text{-Fe}_2\text{O}_3\text{@HAp-Fe}^{2+}$, $\gamma\text{-Fe}_2\text{O}_3\text{@HAp-Ni}^{2+}$, and $\gamma\text{-Fe}_2\text{O}_3\text{@HAp-Ag}$) can be easily prepared. Also, various transition metals such as Ni, Fe, Cd, Zn and Ag are known and versatile among catalysts for organic transformations. $\gamma\text{-Fe}_2\text{O}_3\text{@HAp-Fe}^{2+}$, $\gamma\text{-Fe}_2\text{O}_3\text{@HAp-Ni}^{2+}$, and $\gamma\text{-Fe}_2\text{O}_3\text{@HAp-Ag}$ were used in various organic transformations such as synthesis of pyrano[2,3-d] pyrimidinone derivative [26], chemoselective synthesis of 1,1-diacetate [27], synthesis of the dihydropyrimidinones derivatives [28], regioselective azidolysis of epoxides [29], synthesis of benzimidazoles and benzoxazole derivatives [30], synthesis of tetrahydropyridines [31], and chemoselective oxidation of sulfides to sulfoxides [32].

Having the above subjects in mind, and also in continuation of ongoing program to prepare magnetic nanoparticles or solid acid catalysts and apply them as catalysts in organic synthesis [33, 34], we report a synthesis of new core-shell MNPs having a spherical shape. This $\gamma\text{-Fe}_2\text{O}_3\text{@HAp-Ag}$ NPs is used as an environmentally efficient magnetically recoverable and reusable catalyst for the synthesis of 14-aryl-14H-dibenzo[a,j]xanthenes under solvent-free conditions at 60 °C (Scheme 1).

Experimental

Materials and methods

Reagents and solvents were purchased from Merck, Fluka or Aldrich companies. Melting points were determined in capillary tubes in an electro-thermal C14500 apparatus. The progress of the reaction and the purity of compounds were monitored by TLC using analytical silica gel plates (Merck 60 F250). All known compounds were identified by comparison of their melting points and ^1H NMR and ^{13}C NMR data with those of authentic samples. The ^1H NMR (250 MHz) and ^{13}C NMR (62.9 MHz) spectra were acquired on a Bruker Avance DPX-250, FT NMR spectrometer. IR spectra were recorded on a Frontier FT-IR (Perkin Elmer) spectrometer using KBr disks. The phases present in the magnetic materials were analyzed using powder XRD on a Philips (Holland) spectrometer, model X0 Pert with X' Pert with $\text{CuK}\alpha$ radiation ($\lambda = 1.5401 \text{ \AA}$), with the X-ray generator operated at 40 kV and 30 mA. Diffraction patterns were collected from $2\theta = 20^\circ\text{--}70^\circ$.



Scheme 1. One-pot synthesis of xanthene derivatives in the presence of $\gamma\text{-Fe}_2\text{O}_3\text{@HAp-Ag}$ under solvent-free conditions

Preparation of Ag functionalized on hydroxyapatite-core-shell magnetic $\gamma\text{-Fe}_2\text{O}_3$

In this study, hydroxyapatite-core-shell $\gamma\text{-Fe}_2\text{O}_3$ NPs was prepared according to the literature procedure. Then hydroxyapatite-core-shell $\gamma\text{-Fe}_2\text{O}_3$ NPs (0.6 g) was introduced into 150 mL aqueous solution of silver nitrate (6.7×10^{-3} M) and stirred at room temperature for 6 h. The resulting slurry was filtered, washed, and dried at room temperature in vacuum. Next, the $\gamma\text{-Fe}_2\text{O}_3\text{@HAp}$ NPs containing Ag was treated with an aqueous solution of KBH_4 (5.0×10^{-2} M) for 1 h at room temperature. Again, the slurry was filtered, washed, and dried at room temperature in vacuum, giving Ag functionalized on $\text{Fe}_2\text{O}_3\text{@HAp}$ NPs (Scheme 2). The mean size and the surface morphology of the Ag functionalized on hydroxyapatite-core-shell magnetic $\gamma\text{-Fe}_2\text{O}_3$ were characterized by TEM, SEM, VSM, XRD and FT-IR techniques [35].

Typical procedure for the preparation of 14-aryl-14H-dibenzo[a,j]xanthenes

To a mixture of aldehyde (1 mmol) and 2-naphthol (2 mmol), $\gamma\text{-Fe}_2\text{O}_3\text{@HAp-Ag}$ NPs (15 mg) was added and the mixture was inserted in an oil bath and heated at 60 °C for the appropriate time.

Completion of the reaction was indicated by TLC. After completion of the reaction, the reaction mixture was cooled to room temperature. The reaction mixture was dissolved in ethylacetate and the catalyst was separated out by simple filtration. Excess of solvent was removed under reduced pressure and the crude product was recrystallized with ethanol to afford the pure product in 86–95% yield.

The pH measurement of the silver immobilized on hydroxyapatite-core-shell $\gamma\text{-Fe}_2\text{O}_3$

The determination of pH_{pzc} of sorbent was carried out by pH titration procedure. 50 cm³ of NaCl 0.01 M solution was poured into several erlenmeyer flasks. The pH of solution within each flask was adjusted to a value between 2 and 9 by addition of HCl 0.1 M or NaOH 0.1 M solution. Then, 15 mg of catalyst was added to the flasks and the final pH was measured after 24 h. The pH_{pzc} is defined as the point where the curve pH_{final} vs. $\text{pH}_{\text{initial}}$ crosses the line $\text{pH}_{\text{final}} = \text{pH}_{\text{initial}}$. The point of zero charge of the $\gamma\text{-Fe}_2\text{O}_3\text{@HAp-Ni}^{2+}$ was 6.8.

Results and discussion

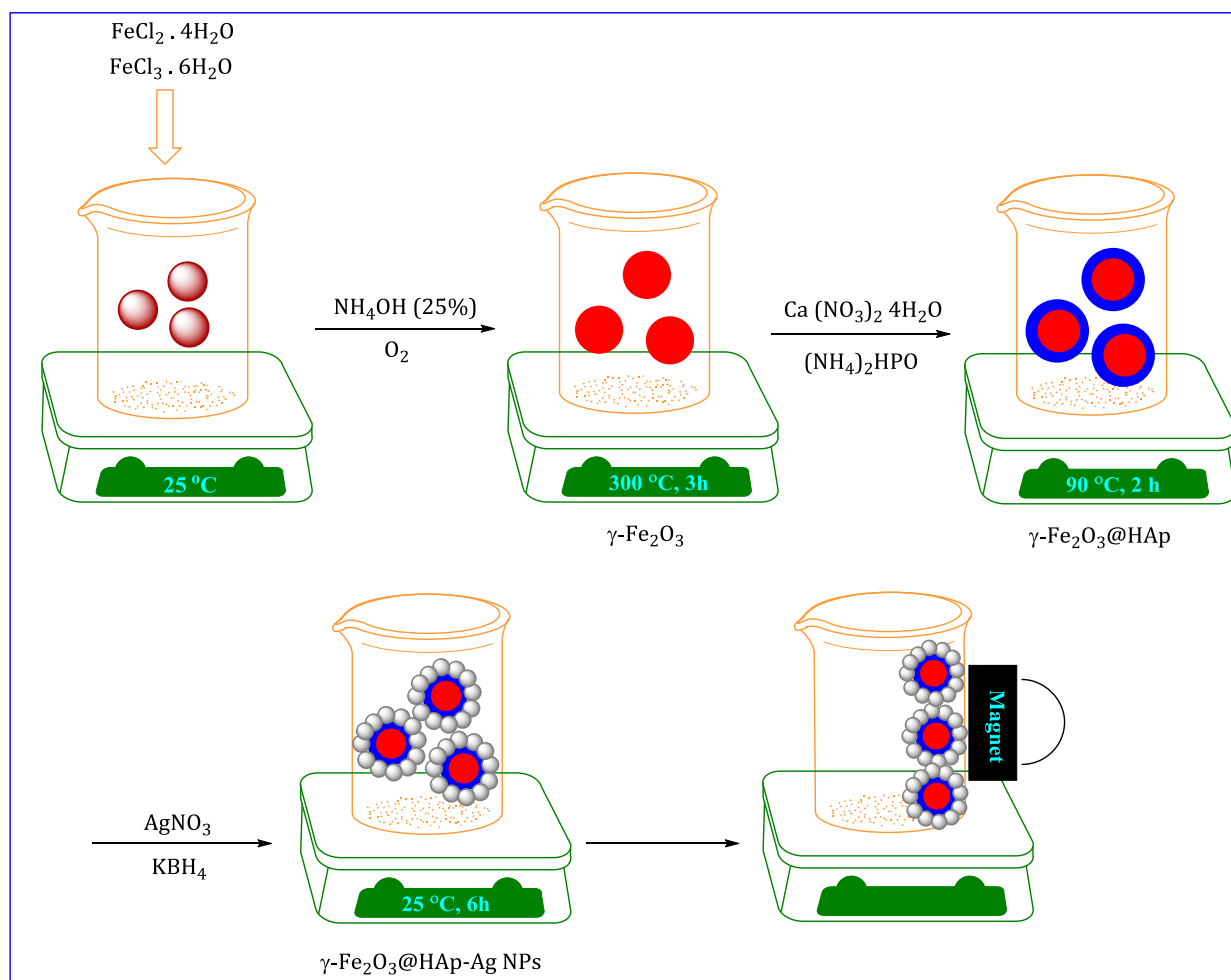
Characterization of catalyst

In recent years, the use of magnetic nanoparticles has many advantages in organic synthesis. For example, high efficiency and selectivity, operational simplicity, environmental compatibility, nontoxic, reusability, low cost, ease of isolation and benefit for industry as well as environment. In this study, the structure of the $\gamma\text{-Fe}_2\text{O}_3\text{@HAp-Ag}$ NPs was characterized by TEM, SEM, VSM, XRD and FT-IR techniques [35].

Silver functionalized on hydroxyapatite-core-shell magnetic $\gamma\text{-Fe}_2\text{O}_3$ nanoparticles ($\gamma\text{-Fe}_2\text{O}_3\text{@HAp-Ag}$) as an environmentally efficient magnetically recoverable and reusable catalyst was reported by *abbasi* et al. and it was used for the 14-aryl-14H-dibenzo[a,j]xanthenes under solvent-free condition.

The scanning electronic microscopy (SEM) image of Ag functionalized on hydroxyapatite-core-shell magnetic $\gamma\text{-Fe}_2\text{O}_3$ nanoparticles is given in [Figure 1](#). As can be clearly seen, the SEM of the $\gamma\text{-Fe}_2\text{O}_3\text{@HAp-Ag}$ NPs showed that the particles of the catalyst were observed in nanosize.

The transmission electronic microscopy (TEM) image of Ag functionalized on hydroxyapatite-core-shell magnetic $\gamma\text{-Fe}_2\text{O}_3$ nanoparticles is given in [Figure 2](#). As can be clearly seen, the TEM micrograph of the $\gamma\text{-Fe}_2\text{O}_3\text{@HAp-Ag}$ NPs clearly proved that the particles were in nanosize. These nanoparticles consist of relatively small, nearly spherical particles, which is nicely consistent with the value obtained from XRD measurements. Also, diameters of approximately 30 nm for the catalyst.



Scheme 2. Schematic representation of the synthesis of $\gamma\text{-Fe}_2\text{O}_3\text{@HAp-Ag NP}$

Figure 1. SEM images of $\gamma\text{-Fe}_2\text{O}_3\text{@HAp-Ag NPs}$

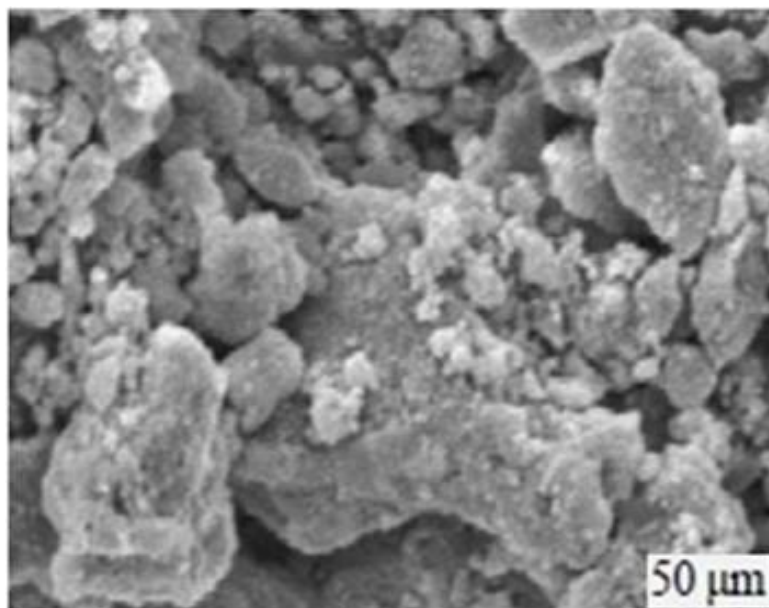
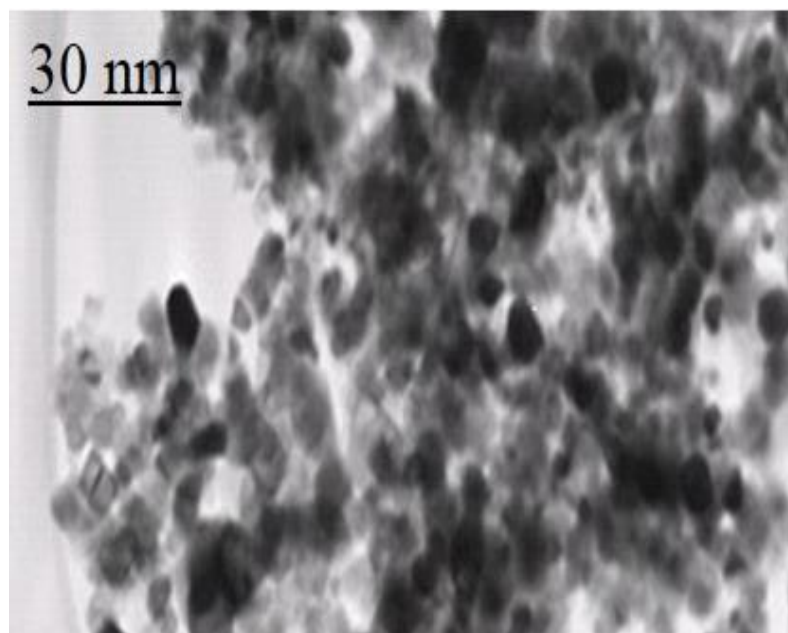


Figure 2. TEM images of γ -Fe₂O₃@HAp-Ag NPs



As shown in [Figure 3](#), X-ray diffraction (XRD) patterns of the synthesized Ag supported on hydroxyapatite-core-shell magnetic γ -Fe₂O₃ nanoparticles display several relatively strong reflection peaks in the 2 θ region of 20°–70°. [Figure 3](#), shows the XRD for Ag functionalized on hydroxyapatite-core-shell magnetic γ -Fe₂O₃ nanoparticles. The crystallinity of the prepared γ -Fe₂O₃@HAp NPs was confirmed by the reflections observed at 2 θ values of 31.2, 32.31, 33.12, 34.32, 45.87 and 49.19. It is also found the metallic Ag phase at 2 θ of 32.19 and 45.32 are found over Ag doped catalysts.

In another investigation, magnetic measurements of Ag functionalized on hydroxyapatite-core-shell magnetic γ -Fe₂O₃ nanoparticles was performed at room temperature using a vibrating sample magnetometer (VSM). The magnetization curve in [Figure 4](#) gives a saturation magnetization value of 13.21 emu/g.

The structural properties of synthesized γ -Fe₂O₃@HAp-Ag MNPs a), HAp supported with Fe₃O₄ MNPs, b) HAp, c) were analyzed by FT-IR spectra ([Figure 5](#)). The band at 3570 cm⁻¹ corresponds to O–H Stretching in the hydroxyapatite structure. The bands at 1095 cm⁻¹, 1025, and 958 corresponds to asymmetric and symmetric stretching vibration of the phosphate group (PO₄³⁻), The peak located at ~ 2344 cm⁻¹ is due to asymmetric stretching C–H. Stretching modes of C–O and C=O are observed at ~ 1388 cm⁻¹ and 1521 cm⁻¹. On doping, stronger and wider absorption bands are observed in the region ~ 1170–698 cm⁻¹ due to the organic capping of silver.

Study of the efficiency of γ -Fe₂O₃@HAp-Ag NPs in the synthesis of 14-aryl-14H-dibenzo[a,j]xanthenes

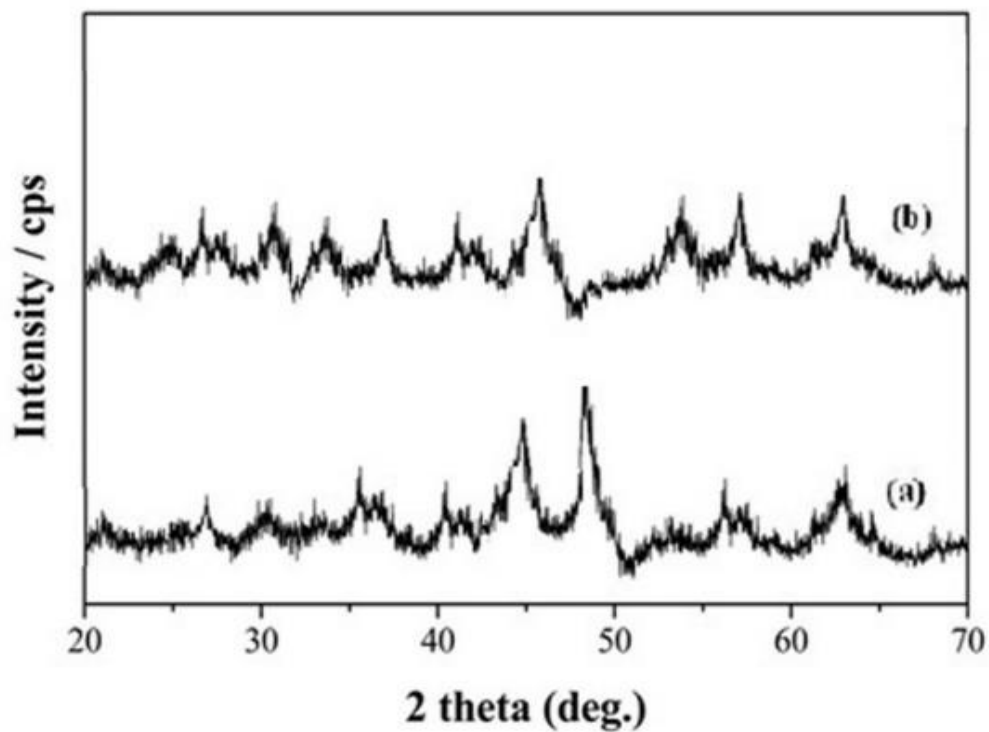


Figure 3. XRD pattern of a) $\gamma\text{-Fe}_2\text{O}_3\text{@HAp}$ and b) $\gamma\text{-Fe}_2\text{O}_3\text{@HAp-Ag NPs}$

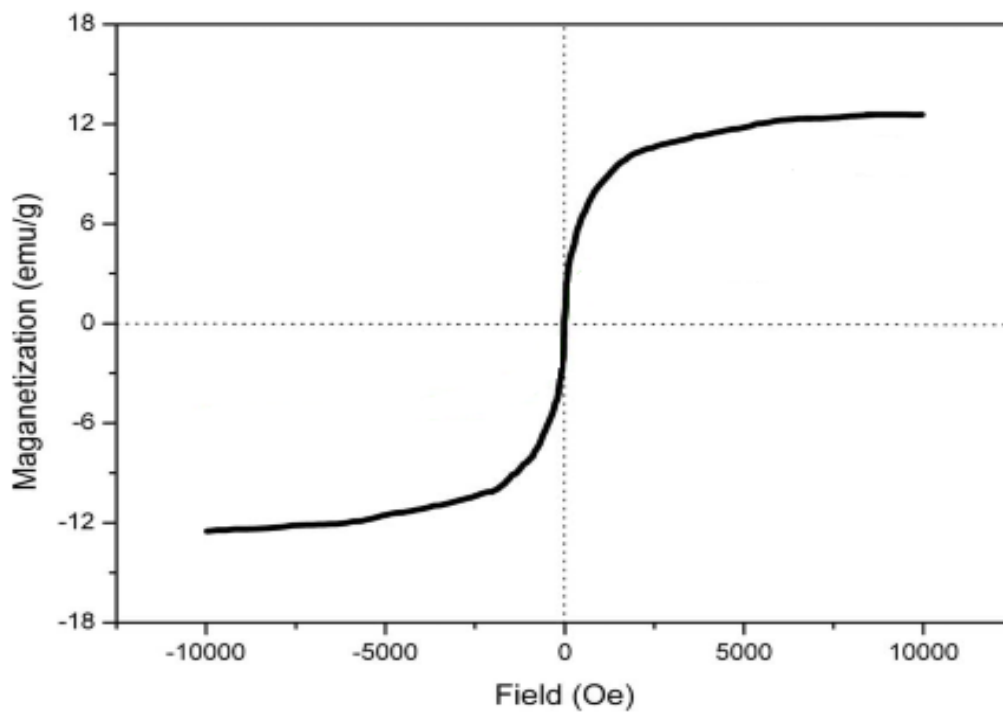


Figure 4. Magnetization curve of $\gamma\text{-Fe}_2\text{O}_3\text{@HAp-Ag NPs}$

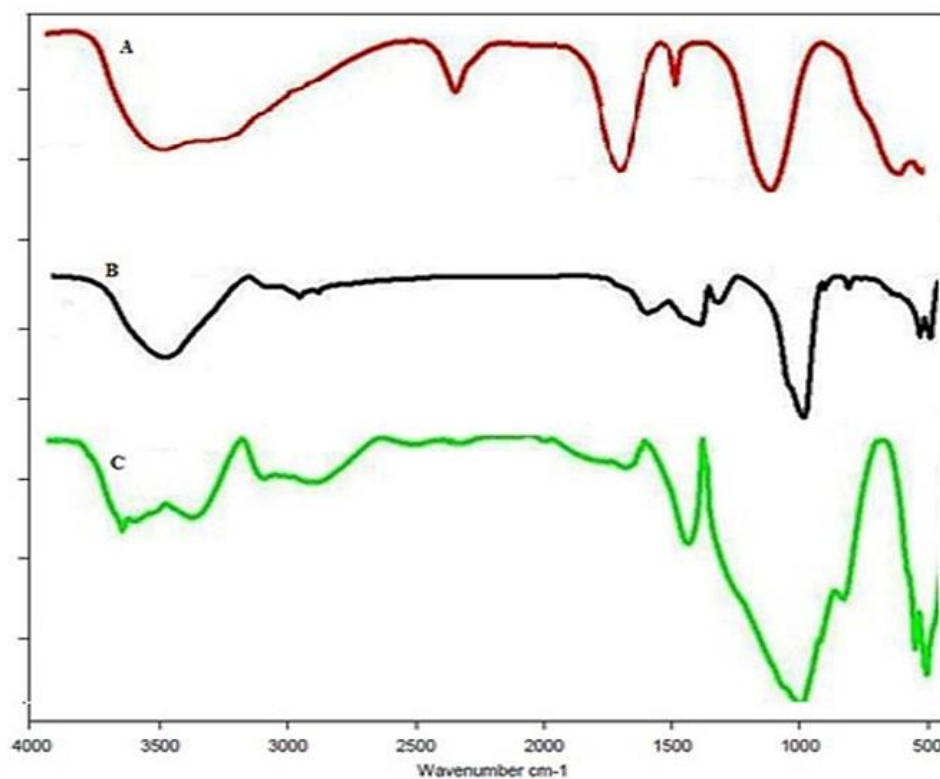


Figure 5. FT-IR spectra of a) $\gamma\text{-Fe}_2\text{O}_3\text{@HAp-Ag NPs}$, b) $\gamma\text{-Fe}_2\text{O}_3\text{@HAp}$, and c) HAp

For this purpose, as a model reaction, the condensation of benzaldehyde (1 mmol) and β -naphthol (2 mmol) was tested using different amounts of $\gamma\text{-Fe}_2\text{O}_3\text{@HAp-Ag NPs}$ at range of 60–100 °C in the absence of solvent (Table 1). As it is shown in Table 1, 15 mg of the catalyst was sufficient to promote the reaction efficiently at 60 °C, and give the product in excellent yield and in short reaction time (Table 1, entry 4).

To compare the efficiency of solution conditions versus the solvent-free procedure, the reaction between benzaldehyde (1 mmol) with β -naphthol (2 mmol) using $\gamma\text{-Fe}_2\text{O}_3\text{@HAp-Ag NPs}$ (15 mg) was checked in some solvents (5 mL) under reflux conditions. The results are summarized in Table 2. As this Table indicates, low yields of the product were obtained in solution conditions even after elongated reaction times.

To assess the efficiency and the scope of $\gamma\text{-Fe}_2\text{O}_3\text{@HAp-Ag NPs}$ in the preparation of 14-aryl-14H-dibenzo[a,j]xanthenes, different aldehydes were reacted with β -naphthol under the optimal reaction conditions; the respective results are displayed in Table 3. As it can be seen in Table 3, both aromatic aldehydes containing electron-donating as well as electron-withdrawing groups were utilized in the present case to form corresponding 14-aryl-14H-dibenzo[a,j]xanthenes in high yields and short

reaction time. However, the reaction conducted by α -naphthol instead of β -naphthol did not afford any product.

Table 1. Effect of the catalyst amount and temperature on the reaction between β -naphthol (1 mmol) with β -naphthol (2 mmol) under solvent-free conditions

Entry	Loading catalyst (mg)	Temperature (°C)	Time (min)	Yield (%) ^a
1	Catalyst-free	-	60	-
2	5	60	50	78
3	10	60	30	81
4	15	60	15	95
5	20	60	20	95
6	25	60	20	91
7	15	80	15	94
8	15	90	15	94
9	15	100	18	92

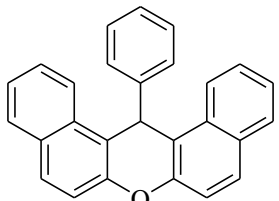
^aYield of isolated products

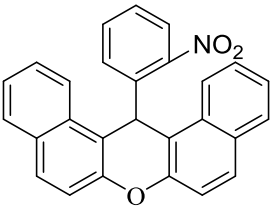
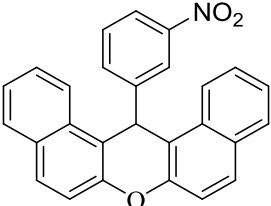
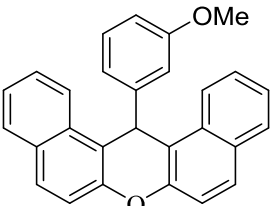
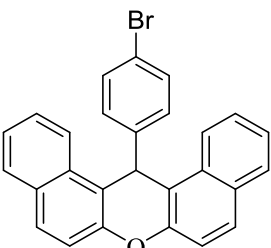
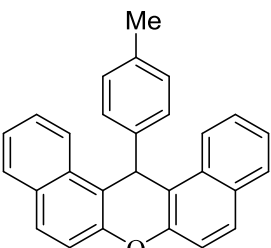
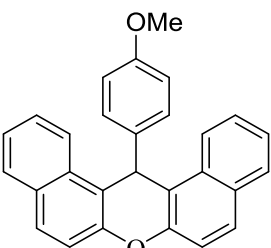
Table 2. Effect of various solvents on the reaction of benzaldehyde (1 mmol) with β -naphthol (2 mmol), in the presence of γ -Fe₂O₃@HAp-Ag NPs (15 mg)

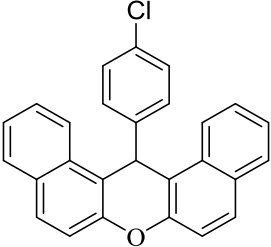
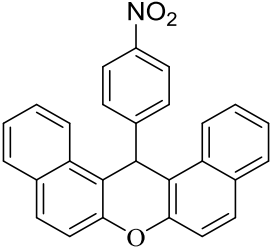
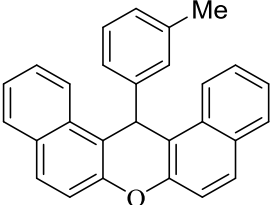
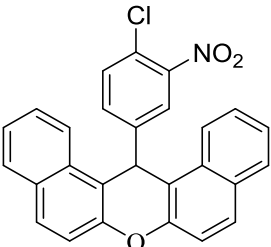
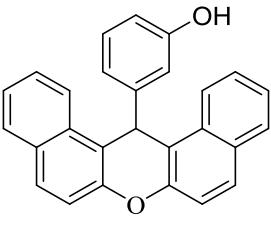
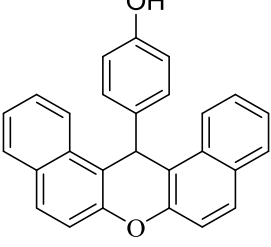
Entry	Solvent	Time (min)	Yield (%) ^a
1	EtOH	45	53
2	CH ₂ Cl ₂	45	4
3	EtOAc	45	50
4	CHCl ₃	45	50
5	H ₂ O	45	45

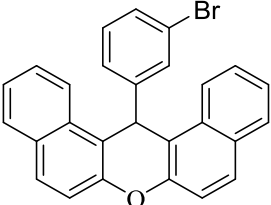
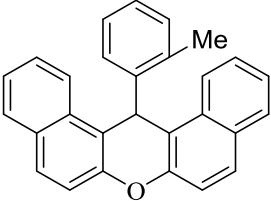
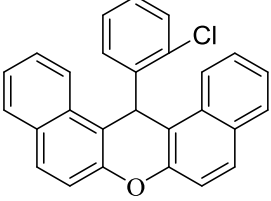
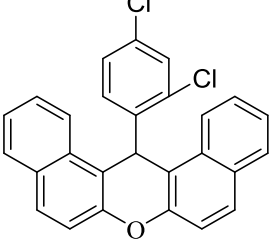
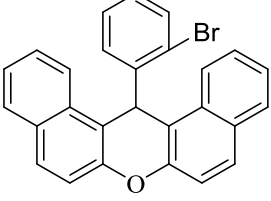
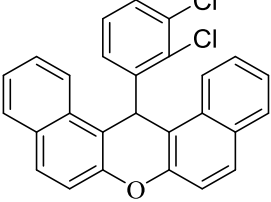
^aYield of isolated products

Table 3. Conversion of aldehyde to xanthene using γ -Fe₂O₃@HAp-Ag NPs under solvent-free condition

Entry	Product	Time (min)	Yield (%) ^a	M.p. (°C) (Lit.)
1		15	95	189-190 191-193 [24]

2		12	91	307-308 309-311 [24]
3		12	94	209-210 210-212 [24]
4		18	86	258-259 260-262 [24]
5		17	95	187-189 186-187 [25]
6		17	92	225-225 226-228 [24]
7		18	89	204-206 203-205 [24]

8		8	94	286-287 285-287 [24]
9		15	92	309-310 310-312 [24]
10		30	91	194-195 195-197 [24]
11		12	90	228-229 230-231 [24]
12		22	90	168-169 169-171 [24]
13		15	91	136-138 138-139 [24]

14		17	92	191-192	193-195 [24]
15		30	89	204-206	205-206 [24]
16		15	94	218-219	219-220 [24]
17		18	95	88-90	87-89 [24]
18		22	89	170-172	169-171 [24]
19		18	91	220-222	221-224 [25]

^aYield of isolated products

In [Table 4](#), our results are compared with the results of any other procedures, for the synthesis of 14-aryl-14H-dibenzo[a,j]xanthenes are described. It is clear that in [Table 4](#) the current method is simpler, more efficient, and less time-consuming for the synthesis of 14-aryl-14H-dibenzo[a,j]xanthene derivatives. The data presented in this table show the comparison between the

promising features of this method in terms of the molar ratio of the catalyst, reaction time and yield of product with those reported in the literature.

The reusability of catalyst is of major importance in green chemistry and also is of major importance for large scale operations and an industrial point of view. Thus the recovery and reusability of γ -Fe₂O₃@HAp-Ag NPs were investigated. From the magnetic separation and isolation of the MNPs catalyst on reaction completion (The reaction between 2-naphthol with benzaldehyde), the additional possibility to reuse and recycle the MNPs catalyst for various runs was too investigated. Results showed in Figure 6 confirm that the magnetically separable MNPs catalyst could be reused and recycled seven runs without any significant loss of its first catalytic activity. In seven runs, the yields of product were 95%, 94%, 94%, 92%, 90%, 88% and 85%, respectively, which verify that the activity of the catalyst remained unchanged throughout these seven runs.

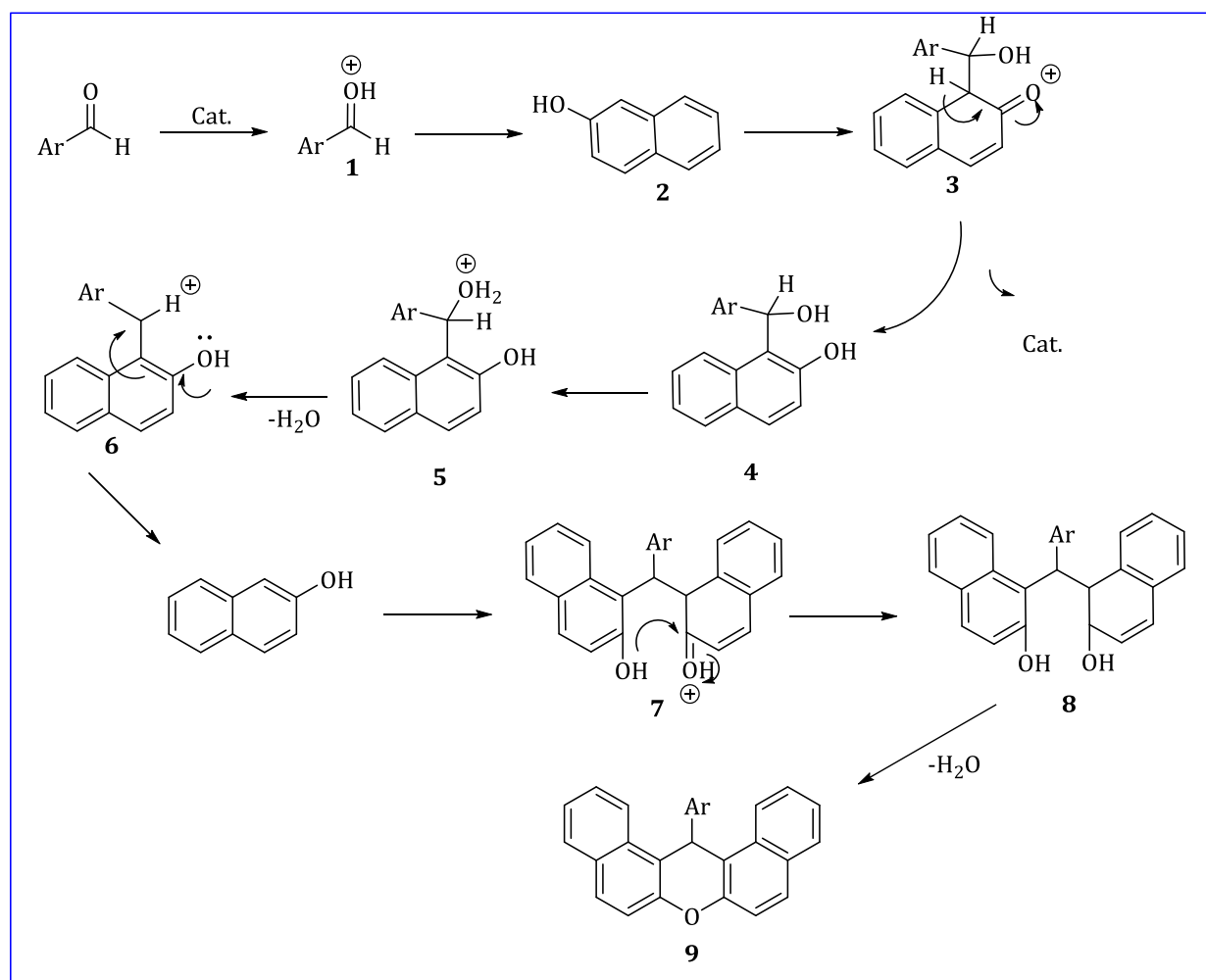
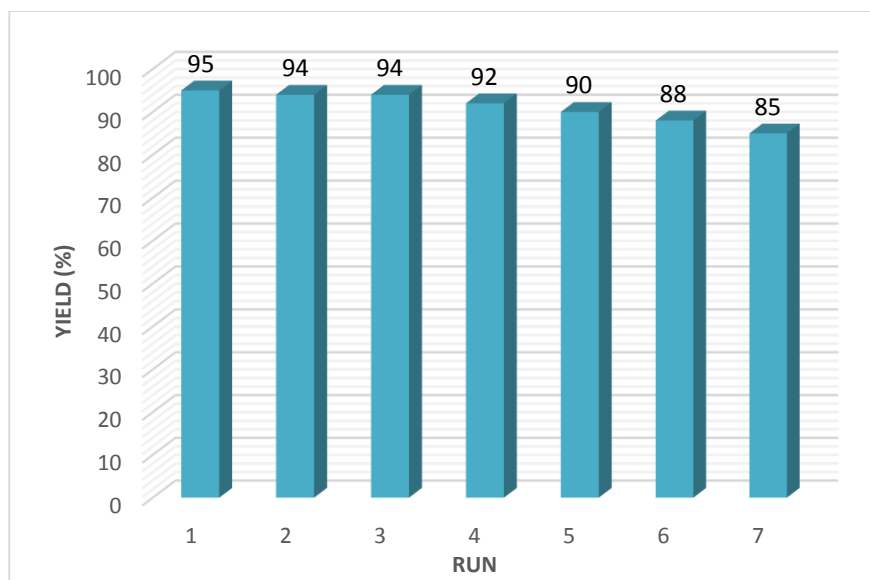
The suggested mechanism for the γ -Fe₂O₃@HAp-Ag NPs catalyzed transformation is shown in Scheme 3. According to the mechanism, γ -Fe₂O₃@HAp-Ag NPs catalyzed the readily in situ formation of 14-aryl-14-H-dibenzo[a,j]xanthenes **9**. The an activated aromatic aldehyde **1** reacts with one molecule of 2-naphthol **2** to provide intermediate **3**, which can be regarded as a fast Knoevenagel addition. Then the active methylene of the second molecule of 2-naphthol reacted with intermediate **3** via conjugate Michael addition to produce the intermediate **7**, which undergoes intramolecular cyclodehydration to give the 14-aryl-14-H-dibenzo[a,j]xanthenes **9**.

Table 4. Comparison of efficiency of various catalysts in synthesis of 14-aryl-14H-dibenzo[a,j]xanthenes

Entry	Catalyst/solvent/temperature	Time (h)	Yield (%)
1	Cellulose sulfuric acid (0.08 g)/ solvent-free/ 110 °C	1.5–3	81–97
2	Amberlyst-15 (1 mmol)/ solvent-free/ 125 °C	0.5–2	80–94
3	Silica sulfuric acid (0.05 g)/ solvent-free/ 80 °C	15–120 ^a	80–96
4	Yb(OTf) ₃ / [BPy]BF ₄ (0.01 mmol)/ 110 °C	5–7	80–95
5	PVPP-BF ₃ / solvent-free (0.05 g)/ 120 °C	1.5–2	92–98
6	ZnO-NPs (0.3 mmol)/ solvent-free/ 150 °C	40–80 ^a	82–92
7	<i>p</i> -Toluene sulfonic acid (0.1 equiv)/ CH ₂ Cl ₂ / reflux	15–24	83–95
8	<i>p</i> -Toluene sulfonic acid (0.1 equiv)/ solvent-free/ 125 °C	2.5–6	80–96
9	PFPAT (10 mol%)/ toluene/ 25-30 °C	3–5	85–97
10	Poly(AMPS-co-AA) (0.04 g)/ solvent-free/ 110 °C	20–30	75–92
11	γ -Fe ₂ O ₃ @HAp-Ag NPs (15 mg)/ solvent-free/ 60 °C	8–30 ^a	86–95

^a In minute

Figure 6. Recoverability of $\gamma\text{-Fe}_2\text{O}_3\text{@HAp-Ag NPs}$



Scheme 3. The plausible mechanism for the condensation reaction of 2-naphthol with aldehydes catalyzed by the $\gamma\text{-Fe}_2\text{O}_3\text{@HAp-Ag NPs}$

Conclusion

In summary, this method is an efficient, economical and 'green' method for the synthesis of xanthenes under solvent-free condition using γ -Fe₂O₃@HAp-Ag NPs as a newly catalyst prepared reagent. This simple method is significant from both environmental and economical point of views as it creates little waste. The important features of this procedure such as excellent yield, short reaction times, non-toxicity of reagent, eco-friendly, simplicity of reaction and reusability of catalyst are the advantages of the present method. The catalyst is readily available, inexpensive and can conveniently be handled and removed from the reaction mixture. This protocol could serve as a valuable alternative to known reactive systems.

Acknowledgments

The authors appreciate the Payame Noor University of Ilam for its financial support to carry out this research.

Orcid

Zeinab Arzehgar  0000-0003-3774-4348

Abdelkarim Aydi  0000-0002-2928-7055

References

- [1]. Omolo J.J., Johnson M.M., van Vuuren S.F., de Koning C.B. *Bioorg Med Chem Lett.*, 2011, **21**:7085
- [2]. Limsuwan S., Trip E.N., Kouwen T.R.H.M., Piersma S., Hiranrat A., Mahabusarakam W., Voravuthikunchai S.P., van Dijn J.M., Kayser O. *Phytomedicine*, 2009, **16**:645
- [3]. Poupelin J.P., Saint-Ruf G., Foussard-Blanpin O., Narcisse G., Uchida-Ernouf G., Lacroix R. *Eur. J. Med. Chem.*, 1978, **13**:67
- [4]. Ahmad M., King T.A., Ko D.K., Cha B.H., Lee J. *J. Phys. D: Applied Physics*, 2002, **35**:1473
- [5]. Knight C.G., Stephens T. *Biochem. J.*, 1989, **258**:683
- [6]. Kitahara Y., Tanaka K. *Chem. Commun.*, 2002, 932 DOI:10.1039/B110514K
- [7]. Nagarapu L., Kantevari S., Mahankhali V.C., Apuri S. *Catal. Commun.*, 2007, **8**:1173
- [8]. Pasha M.A., Jayashankara V.P. *Bioorganic Med. Chem. Lett.*, 2007, **17**:621
- [9]. Bigdeli M.A., Heravi M.M., Mahdavinia G.H. *J Mol Catal A: Chem.*, 2007, **275**:25
- [10]. Patil S.B., Bhat R.P., Samant S.D. *Synth. Commun.*, 2006, **36**:2163
- [11]. Wang J.Q., Harvey R.G. *Tetrahedron*, 2002, **58**:5927
- [12]. Knight D.W., Little P.B. *Synlett*, 1998, **10**:1141
- [13]. Kuo C.W., Fang J.M. *Synth. Commun.*, 2001, **31**:877

- [14]. Jha A, Beal J. *Tetrahedron Lett.*, 2004, **45**:8999
- [15]. Rao G.B.D., Kaushik M.P., Halve A.K. *Tetrahedron Lett.*, 2012, **53**:2741
- [16]. Kumar P.S., Sreenivasulu N., Sunil Kumar B., Rajitha B., Narsimha Reddy P., Thirupathi Reddy Y. *Arkivoc*, 2006, **xii**:46
- [17]. Rajitha B., Sunil Kumar B., Thirupathi Reddy Y., Narsimha Reddy P., Sreenivasulu N. *Tetrahedron Lett.*, 2005, **46**:8691
- [18]. Nazari S., Keshavarz M., Karami B., Irvani N., Vafae-Nezhad M. *Chin. Chem. Lett.*, 2013, **25**:317
- [19]. Shirini F., Ghaffari Khaligh N. *Dyes Pigm.*, 2012, **95**:789
- [20]. Dabiri M., Azimi S.C., Bazgir A. *Chem. Pap.*, 2008, **62**:522
- [21]. Zolfigol M.A., Khakyzadeh V., Moosavi-Zare A.H., Zare A., Azimi S.B., Asgari Z., Hasaninejad A.R. *C. R. Chim.*, 2012, **15**:719
- [22]. Shaterian H.R., Ghashang M.J. *Braz. Chem. Soc.*, 2008, **19**:1053
- [23]. Rezayati S., Mirzajanzadeh E., Seifournia H. *Asian J. Green Chem.*, 2017, **1**:24
- [24]. Haeri H.S., Rezayati S., Rezaee Nezhad E., Darvishi H. *Res. Chem. Intermed.*, 2016, **42**:4773
- [25]. Moosavi-Zare A.R., Zolfigol M.A., Zare M., Zare A., Khakyzadeh V. *Journal Molecular Liquids*, 2015, **211**:373
- [26]. Rezayati S., Abbasi Z., Rezaee Nezhad E., Hajinasiri R., Farrokhnia A. *Res. Chem. Intermed.*, 2016, **42**:7597
- [27]. Rezaee Nezhad E., Sahhadifar S., Abbasi Z., Rezayati S. *J. Sci. I. R. Iran*, 2004, **25**:127
- [28]. Rezaee Nezhad E., Abbasi Z., Sajjadifar S. *Sci. Iran.*, 2015, **22**:903
- [29]. Sajjadifar S., Abbasi Z., Rezaee Nezhad E., Rahimi Moghaddam M., Karimian S., Miri S. *J. Iran Chem. Soc.*, 2014, **11**:335
- [30]. Rezayati S., Abbasi Z., Rezaee Nezhad E., Hajinasir R., Soleymani Chalanchi Sh. *Org. Chem. Res.*, 2016, **2**:162
- [31]. Sajjadifar S., Rezayati S., Shahriari A., Abbaspour S. *Appl. Organometal. Chem.*, 2017, <https://doi.org/10.1002/aoc.4172>
- [32]. Sajjadifar S., Rezayati S., Arzehgar Z., Abbaspour S., Torabi Jafroudi M. *J. Chin. Chem. Soc.*, 2018, <https://doi.org/10.1002/jccs.201800036>
- [33]. Soleiman-Beigi M., Arzehgar Z. *Monatsh Chem.*, 2016, **147**:1759
- [34]. Sajjadifar S., Arzehgar Z., Ghayuri A. *J. Chin. Chem. Soc.*, 2018, **65**:205
- [35]. Abbasi Z., Rezayati S., Bagheri M., Hajinasiri R. *Chin. Chem Lett.*, 2017, **28**:75

How to cite this manuscript: Zeinab Arzehgar*, Abdelkarim Aydi, Mohammad Mirzaei Heydari. Silver functionalized on hydroxyapatite-core-shell magnetic γ -Fe₂O₃: An environmentally and readily recyclable nanocatalyst for the one-pot synthesis of 14H-dibenzo[a,j]xanthenes derivatives. *Asian Journal of Green Chemistry*, 2018, 2, 281-298. DOI: [10.22034/ajgc.2018.61867](https://doi.org/10.22034/ajgc.2018.61867)